Multi-model simulations of aerosol and ozone radiative forcing due to anthropogenic emission changes during the period 1990-2015

Article

www.reading.ac.uk/centaur

CentAUR

Central Archive at the University of Reading

Reading's research outputs online

Atmospheric
Chemistry
and Physics

Multi-model simulations of aerosol and ozone radiative forcing due to anthropogenic emission changes during the period 1990–2015

Gunnar Myhre[1], **Wenche Aas**[2], **Ribu Cherian**[3], **William Collins**[4], **Greg Faluvegi**[5], **Mark Flanner**[6], **Piers Forster**[7], **Øivind Hodnebrog**[1], **Zbigniew Klimont**[8], **Marianne T. Lund**[1], **Johannes Mülmenstädt**[3], **Cathrine Lund Myhre**[2], **Dirk Olivié**[9], **Michael Prather**[10], **Johannes Quaas**[3], **Bjørn H. Samset**[1], **Jordan L. Schnell**[10], **Michael Schulz**[9], **Drew Shindell**[11], **Ragnhild B. Skeie**[1], **Toshihiko Takemura**[12], and **Svetlana Tsyro**[9]

[1]Center for International Climate and Environmental Research – Oslo (CICERO), Oslo, Norway
[2]NILU – Norwegian Institute for Air Research, Kjeller, Norway
[3]Institute for Meteorology, Universität Leipzig, Leipzig, Germany
[4]Department of Meteorology, University of Reading, Reading, UK
[5]NASA Goddard Institute for Space Studies and Center for Climate Systems Research, Columbia University, New York, USA
[6]Department of Climate and Space Sciences and Engineering, University of Michigan, Ann Arbor, MI, USA
[7]School of Earth and Environment, University of Leeds, Leeds, UK
[8]International Institute for Applied Systems Analysis (IIASA), Laxenburg, Austria
[9]Norwegian Meteorological Institute, Oslo, Norway
[10]Department of Earth System Science, University of California, Irvine, CA 92697-3100, USA
[11]Nicholas School of the Environment, Duke University, Durham, NC 27708, USA
[12]Research Institute for Applied Mechanics, Kyushu University, Fukuoka, Japan

Correspondence to: Gunnar Myhre (gunnar.myhre@cicero.oslo.no)

Abstract. Over the past few decades, the geographical distribution of emissions of substances that alter the atmospheric energy balance has changed due to economic growth and air pollution regulations. Here, we show the resulting changes to aerosol and ozone abundances and their radiative forcing using recently updated emission data for the period 1990–2015, as simulated by seven global atmospheric composition models. The models broadly reproduce large-scale changes in surface aerosol and ozone based on observations (e.g. -1 to $-3\%\,\mathrm{yr}^{-1}$ in aerosols over the USA and Europe). The global mean radiative forcing due to ozone and aerosol changes over the 1990–2015 period increased by $+0.17 \pm 0.08\,\mathrm{W\,m}^{-2}$, with approximately one-third due to ozone. This increase is more strongly positive than that reported in IPCC AR5. The main reasons for the increased positive radiative forcing of aerosols over this period are the substantial reduction of global mean SO_2 emissions, which is stronger in the new emission inventory compared to that used in the IPCC analysis, and higher black carbon emissions.

1 Introduction

Over the last decades, global temperature has been forced by a range of both natural and anthropogenic drivers (Schmidt et al., 2014b; Solomon et al., 2011). Relative to the period 1984–1998, which ended with a strong El Niño, the period 1998–2012 saw a reduced rate of global warming. A wide range of studies have discussed possible causes of this slowdown (Fyfe et al., 2016; Marotzke and Forster, 2015; Nieves et al., 2015), including discussions of the temperature trend itself (Karl et al., 2015). A record surface temperature over the instrumental period was however reached in 2014 (Karl et al., 2015), with another new record in 2015. Understanding the reasons behind periods with weaker or stronger temperature changes superimposed on the long-term trend in temperature that is continually forced by increased greenhouse gas concentrations is an integral part of the general study of the climate system.

The Intergovernmental Panel on Climate Change (IPCC) Fifth Assessment Report (AR5) had to rely on a limited number of studies for the 1998–2011 period with regard to radiative forcing of short-lived components (Flato et al., 2013; Myhre et al., 2013b). The short-lived components, notably ozone and atmospheric aerosols, are more difficult to quantify in terms of abundance and radiative forcing through atmospheric measurements than the greenhouse gases with lifetimes on the order of decades or longer. Abundances of short-lived components depend on location of emission and are inhomogeneously distributed in the atmosphere, with variability in time, geographical distribution and altitude.

The short-lived compounds of particular importance in terms of radiative forcing include ozone and atmospheric aerosols. Over the last decades, large changes in regional emissions of ozone and aerosol precursors have occurred, with reductions over the USA and Europe in response to air quality controls, and a general increase over southern and eastern Asia (Amann et al., 2013; Crippa et al., 2016; Granier et al., 2011; Klimont et al., 2013). The available emission data for various aerosol types differ in magnitude across regions (Wang et al., 2014b). The net effect of these emission changes in terms of changes in the Earth's radiative balance is not obvious. In addition to a change in the geographical location of the emissions that emphasises more chemically active, low-latitude regions, different types of aerosols have different impacts on the radiative balance. Some are purely scattering, while others enhance absorption of solar radiation. They may also affect cloud formation, albedo and lifetime through a range of mechanisms (Boucher et al., 2013; Kaufman et al., 2002). Since the net aerosol forcing is negative (cooling), a reduction in anthropogenic primary aerosol emissions and emissions of aerosol precursors implies a positive forcing over the time period of emission reductions.

The aerosols have a variety of types and composition and involve several different forcing mechanisms, specifically aerosol–radiation interactions (previously denoted direct aerosol effect and semi-direct effect when allowing for rapid adjustments) and aerosol–cloud interactions (Boucher et al., 2013). Their forcing over the industrial era has substantial uncertainties, quantified in terms of a total aerosol forcing of -0.9 (-1.9 to -0.1) $W\,m^{-2}$ (Boucher et al., 2013). The IPCC AR5 mainly relied on Shindell et al. (2013a) for changes over the last 1–2 decades for the total aerosol forcing, in addition to one study for the direct aerosol effect based on satellite data (Murphy, 2013). The model studies available for the 2000-2010 period based on the results in Shindell et al. (2013a) were few compared to what was available for earlier time periods. These studies revealed large regional changes in the aerosol forcing over the last decades, but in terms of global mean changes the values were small in magnitude. The clear sky direct aerosol effect over the period 2000–2012 showed small global mean forcing based on the changes in aerosol abundance from MISR satellite data (Murphy, 2013). The total aerosol forcing over

the period 1990–2010 and 2000–2010 in IPCC AR5 was quantified as -0.03 and $+0.02$ $W\,m^{-2}$, respectively (Myhre et al., 2013b). Tropospheric ozone forcing was estimated to be $+0.03$ $W\,m^{-2}$ over the 1990–2010 period. Kuhn et al. (2014) simulated a weak direct aerosol effect forcing of $+0.06$ $W\,m^{-2}$ over the 1996–2010 period, but with a much stronger forcing of $+0.42$ $W\,m^{-2}$ for the total aerosol effect.

At present, aerosol forcing is diagnosed using a wide range of methods, with various degrees of sophistication of the aerosol–radiation and aerosol–cloud interactions included. To span this range and take different approaches into account, we encouraged the modelling groups participating in this study to perform aerosol and ozone forcing simulations over the 1990–2015 period with their standard configuration, but using updated emission inventories and more consistent diagnostics. Here, we present the resulting evolution of aerosol and ozone abundances at the regional level and the resulting radiative forcing. In particular, the aim is to quantify the recent changes in radiative forcing and how those compare to the values reported in the IPCC AR5.

2 Methods

The seven global models participating in the present study are described in Table 1. Participating modelling groups are from the European Union project ECLIPSE[1] (Stohl et al., 2015) and those joining an open call for collaborating groups. The model set-up to derive forcing varies between the models: from fixed meteorology, to one meteorological year, to fixed sea surface temperatures. All models use identical anthropogenic emission data from ECLIPSE for the 1990 to 2015 period (Klimont et al., 2016; Stohl et al., 2015). Several updates and improvements compared to earlier emission data sets were included in this inventory (Klimont et al., 2016). The ECLIPSE emission data are shown in Fig. 1 over the period 1990–2015 and are compared to emission data used in Coupled Model Intercomparison Project Phase 5 (CMIP5) and to be used in CMIP6. Figure S1 in the Supplement show emission data over Europe and south-eastern Asia, respectively. Black carbon (BC) emissions are higher in the ECLIPSE data compared to the CMIP5 data, but with similar trends. For SO_2 emission, the former has a somewhat larger reduction towards the end of the 1990–2015 period than in the CMIP5 data. For the Community Emissions Data System (CEDS) data for CMIP6, the largest change to the ECLIPSE data is the more pronounced increase in NO_x and organic carbon (OC) for the end of the 1990 to 2015 period. The CEDS data will be explored through a large set of simulations within CMIP6 (Eyring et al., 2016).

All models simulated the main anthropogenic components sulfate, black carbon and primary organic aerosols (POA).

---

[1]Evaluating the Climate and Air Quality Impacts of Short-Lived Pollutants (ECLIPSE); European Union Seventh Framework Programme (FP7/2007-2013) under grant agreement no. 282688.

Table 1. Model description.

Models	Resolution	Fixed met or fixed sea surface temperature (SST)	Rapid adjustment	Anthropogenic aerosol components included	References
CESM (CAM5, MAM3, MOZART)	1.9° × 2.5° L30	1982–2001 climatological monthly varying fixed SSTs and sea ice	No (direct effect only)	Sulfate, BC, POA, SOA	Liu et al. (2012); Neale et al. (2010); Wang et al. (2013)
ECHAM6-HAM2	T63 (1.8 × 1.8), L31	Climatological monthly varying fixed SST and sea ice extent averaged for the period 1979 to 2008	Included for semi-direct effect, cloud–aerosol interactions on liquid water clouds (no parameterised effects on ice clouds or convective clouds)	Sulfate, BC, POA	Stevens et al. (2013); Zhang et al. (2012)
EMEP	0.5° × 0.5° L20	2010 met	Included for semi-direct effect of BC (CESM-CAM4)	Sulfate, nitrate, BC, POA, SOA	Simpson et al. (2012)
GISS	2.0° × 2.5° L40	2000 climatological monthly varying fixed SSTs and sea ice	Yes	Sulfate, BC, POA, SOA, nitrate (dust also influenced by other anthropogenic aerosols)	Schmidt et al. (2014a); Shindell et al. (2013b)
NorESM1	1.9° × 2.5° L26	Climatological monthly varying fixed SSTs and sea ice extent over the 1990–2013 period	No	Sulfate, BC, POA (SOA included in POA)	Bentsen et al. (2013); Iversen et al. (2013); Kirkevåg et al. (2013)
OsloCTM2	T42 2.8° × 2.8° L60	2010 met	Included for semi-direct effect of BC (CESM-CAM4)	Sulfate, BC, POA, SOA, nitrate	Myhre et al. (2009); Skeie et al. (2011)
SPRINTARS	1.125° × 1.125° L56	Climatological monthly varying fixed SSTs and sea ice extent over the 1988–1992 period	Included	Sulfate, BC, POA, SOA	Takemura et al. (2005, 2009)

Furthermore, some models include secondary organic aerosols (SOA) and nitrate. Five of the models simulated ozone changes over the period. The same offline radiative transfer code used for calculating the radiative forcing for OsloCTM2 was adopted for the atmospheric abundance changes from the EMEP model.

Differences in atmospheric abundances can be large due to different meteorological data sets (up to more than 50 % in global mean aerosol burden) (Liu et al., 2007), and sur-
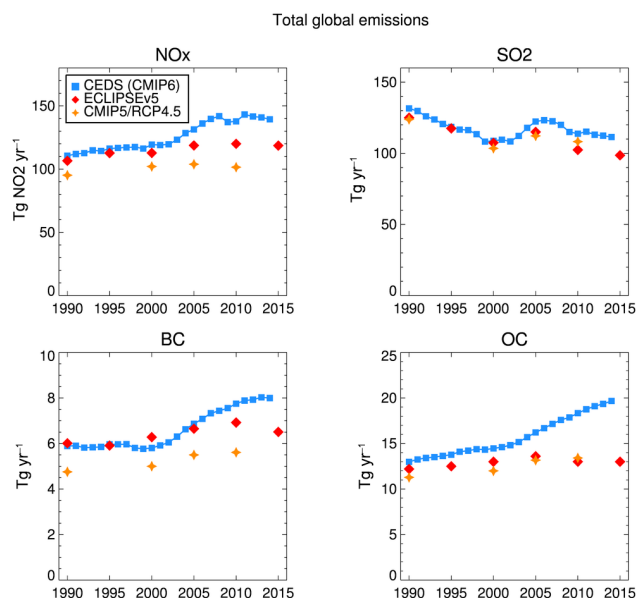
Figure 1. Global mean emissions for NO_x, SO_2, BC and OC for ECLIPSE (Klimont et al., 2016), data applied in Coupled Model Intercomparison Project (CMIP5) (Lamarque et al., 2010), and Community Emissions Data System (CEDS) to be used in CMIP6 (Hoesly et al., 2017) over the period 1990–2015.

Figure 2. Multi-model mean linear change in surface $PM_{2.5}$ **(a)** and aerosol optical depth (AOD) at 550 nm **(b)**, over the 1990–2015 period, simulated by the six models GISS, OsloCTM2, NorESM, CESM-CAM5, EMEP and SPRINTARS.

face concentrations can be influenced by interannual variation (making 20-year trends in surface ozone due to climate variability as large as caused by changes in emission ozone precursors) (Barnes et al., 2016), but differences associated with nudging seem to be small (a few percentage points) (Sand et al., 2017).

The forcing calculations are quantified at the top of the atmosphere for aerosols and at the tropopause for ozone and follow definitions made in IPCC AR5 (Boucher et al., 2013; Myhre et al., 2013b). The consideration of rapid adjustments associated with aerosols for the various models is described in Table 1.

Radiative forcing is defined as a perturbation relative to a reference state; this can be a flexible year and most common to pre-industrial time (Boucher et al., 2013; Myhre et al., 2013b). All the aerosol and ozone forcings shown here are absolute changes ($W\,m^{-2}$) relative to the 1990 value of each model. Thus, all the plots show forcing starting at 0.0 in 1990.

3 Results

3.1 Trends in aerosol and ozone

Evaluation of aerosol and chemistry models is a huge topic, given the large spatial variability in aerosol and chemical species as well as the difficulties associated with sampling issues (Schutgens et al., 2016) and the availability of long-
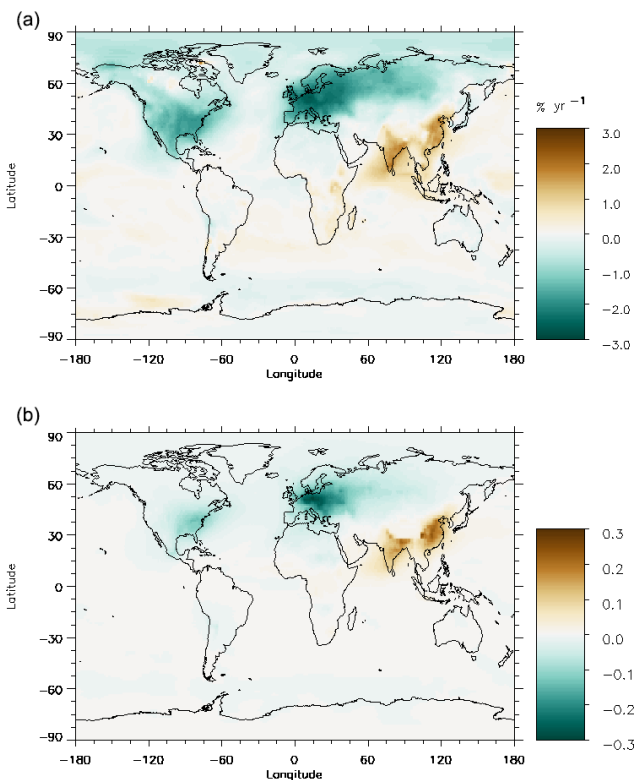
term measurements. In this study we restrict the comparison between the models and observations to surface fine-mode particular matter, which we further show to have a similar trend as the total column aerosol optical depth (AOD). In the Supplement we show comparison of surface ozone between the models used in this study and observations. In addition, Fig. S2 presents trends in the tropospheric column and surface ozone from the models, showing a much larger difference between surface and column than for aerosols. Whereas the forcing efficiency of aerosols is strongly dependent on the surface reflectance and their position in relation to clouds (Haywood and Shine, 1997), the forcing efficiency for ozone is strongly dependent on altitude and is most efficient around tropopause altitude (Forster and Shine, 1997; Lacis et al., 1990; MacIntosh et al., 2016).

Six models simulated changes in annually averaged $PM_{2.5}$ (particulate matter with aerodynamic diameters less than 2.5 μm) over the 1990–2015 period. A model mean linear trend is fitted and shown as a function of latitude and longitude; see Fig. 2a. Regional changes in the model mean range from 2 to $3\,\%\,yr^{-1}$ reductions over much of the USA and Europe to 1 to $2\,\%\,yr^{-1}$ increases over much of southern and eastern Asia. The inter-model variation is small, as the models simulate broadly similar geographical patterns. Ob-

Table 2. Change in PM$_{2.5}$ given in % yr^{-1} over Europe and the USA for observations and multi-model mean. Values in parentheses are standard deviations of the observed trends. Models were sampled at the grid points of the network sites. For the models, periods 2000–2010 and 1990–2010 were used for comparisons with US observations.

	# sites	Observations (% yr^{-1})	Mean models (% yr^{-1})
Europe 2000–2010, based on EMEP network[a]	13	−2.9 (1.5)	−2.4
USA 2000–2009, based on IMPROVE network[b]	153	−2.1 (2.07)	−1.9
USA 1989–2009, based on IMPROVE network[b]	59	−1.5 (1.25)	−1.3

[a] Modified from Tørseth et al. (2012) by extending 1 additional year. Same trend methods are used. [b] Adapted from Hand et al. (2011).

servations of changes in PM$_{2.5}$ based on the atmospheric networks EMEP (Europe) and IMPROVE (USA) are available for selected time periods. The PM$_{2.5}$ trends from observations and model mean results are compared in Table 2. The model results were derived at the model grid of the observational sites. Over Europe the observed trend is limited to the decade 2000–2010 and is −0.5 % yr^{-1} larger (more negative) than the model mean (see Tørseth et al., 2012 for description, site selection and trend methods). Over the USA we have two decades of PM$_{2.5}$ data, 1998–2008 (Hand et al., 2011, 2014). We compare with the 2000s decade for consistency with the EMEP comparison and with the 1989–2008 observations for a longer record. The US record shows that greater per cent reductions occurred in the second decade, and this is matched by the model simulations. Consistent with the European record, the observations are −0.2 % yr^{-1} more negative than models over either period. Thus, our simulation appears to slightly underestimate the reductions in PM$_{2.5}$ over the USA and Europe. In Fig. 2b the AOD at 550 nm is shown as model mean trend in absolute AOD, similar to PM$_{2.5}$ in Fig. 2a. Maximum reduction in AOD is 0.30 (absolute AOD) over Europe and maximum increase is 0.25 over eastern Asia.

Five models simulated surface ozone changes based on the prescribed emissions of precursors, including methane. The resulting annual mean surface ozone change (absolute, in ppb) from 1990 to 2015 is shown in Fig. S2. The pattern of ozone change is similar among the models, but with some differences in magnitude. The regional changes in surface ozone have many similarities with the surface PM$_{2.5}$ changes (Fig. 2). Surface ozone increases are seen along maritime shipping routes due to increased NO$_x$ emissions. Figures S3 and S4 and Table S1 in the Supplement show the surface changes (ppb decade^{-1}) from the models compared to observations over the USA and Europe. Extensive networks of surface ozone measurements, using the full 2000 or so air quality sites in both the USA and Europe, are available from 1993 (USA) and 1997 (Europe) up to the cut-off date of 2013 (see Schnell et al., 2014 2015 for networks and methods). These gridded observations identify small-scale variations in the geographic pattern of ozone trends, which are only par-
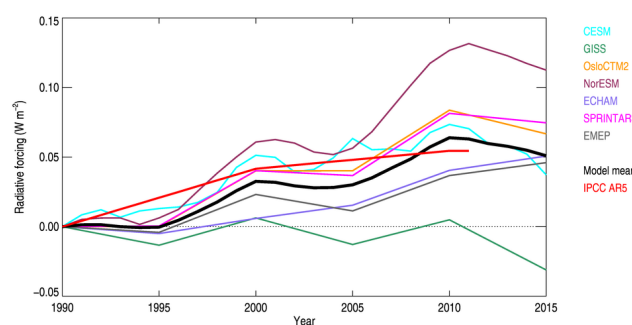

Figure 3. Radiative forcing (W m^{-2}) of the direct aerosol effect over the period 1990–2015 given for seven models (legend lists the models); the multi-model mean is shown in black and the estimate provided in IPCC AR5 is included in red.

tially captured in these simulations. Some of the models capture some of the main seasonal shifts (e.g. decrease in summer peak ozone with increase in winter ozone over the eastern USA and Europe).

3.2 Direct aerosol effect

The total global annual mean radiative forcing of the change since 1990 in direct aerosol effect is shown in Fig. 3 for seven models, together with the estimate given in IPCC AR5. The model mean is very close to the IPCC AR5 value, but the model spread is large. The model mean direct aerosol effect has a positive forcing in the periods 1995–2000 and 2005–2010, with the forcing over the other 5-year periods being negative or consistent with zero.

The model range for the direct aerosol effect due to changes in sulfate concentrations is smaller than that for the total direct aerosol effect; see Fig. 4a. The range for sulfate forcing is a factor of 2, slightly lower than the model range from other recent multi-model studies (Myhre et al., 2013a). The differences in sulfate burdens between a much larger group of models in IPCC AR5 was greater (Prather et al., 2013). In all of multi-model analyses, differences are not simply proportional to burden because radiative forcing is calculated with different assumptions of optical properties
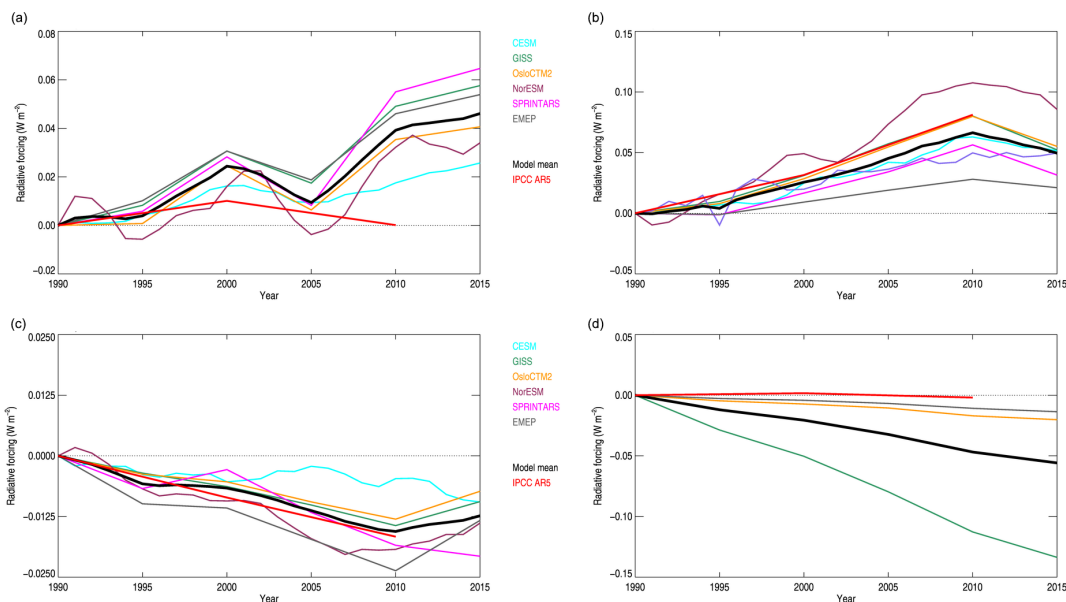
Figure 4. Radiative forcing (W m^{-2}) of the direct aerosol effect by aerosol component (sulfate, **a**; BC, **b**; POA, **c**; nitrate, **d**) over the period 1990–2015.
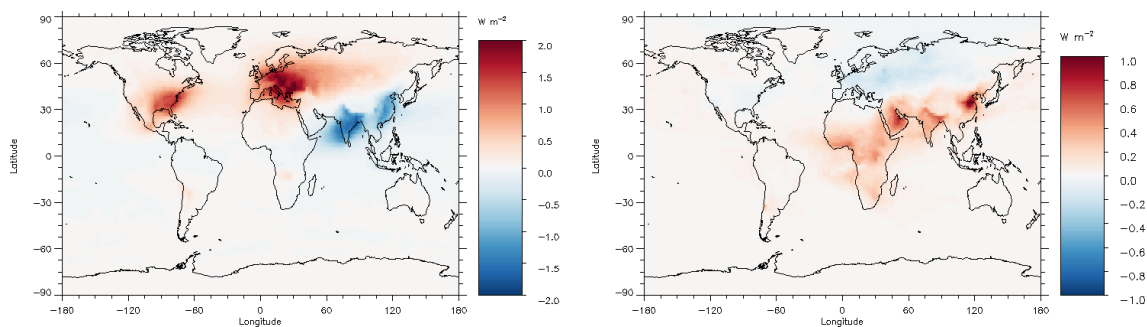

Figure 5. Geographical distribution of the 1990–2015 radiative forcing (W m^{-2}) of the multi-model mean direct aerosol effect sulfate (left panel) and BC (right panel) as driven by emission changes.

and because of the importance of the host model for radiative transfer calculations and background fields of factors such as clouds and surface albedo (Myhre et al., 2013a; Stier et al., 2013). The IPCC AR5 estimate for direct aerosol effect of sulfate was close to zero for the whole 1990–2010 period, whereas the multi-model mean here is around $+0.04$ W m^{-2} in the year 2010, with further increase to $+0.05$ W m^{-2} in 2015. A main reason for this difference is that in the new ECLIPSE emission inventory, global sulfate precursor emissions show stronger reductions for this period than previous estimates. The ECLIPSE SO$_2$ emission change over the 1990–2015 period is about -20 %, including international shipping (Klimont et al., 2016; Stohl et al., 2015). Despite the overall positive direct aerosol forcing of sulfate over the 1990–2015 period from a global reduction of sulfate, it is negative in the intermediate 5-year period 2000–2005.

The model mean global mean radiative forcing of BC direct aerosol effect increases over the 1990–2010 period by $+0.07$ W m^{-2} (see Fig. 4b), with values about 20 % lower than in IPCC AR5. Between 2010 and 2015 the multi-model mean drops by 25 %. The model spread for BC is generally somewhat larger than for sulfate, where differences in the modelled BC vertical profile are the main contributors (Hodnebrog et al., 2014; Samset et al., 2013). The BC emission increases from 1990 to 2015 are 10 % in the global sum, but the increase in radiative forcing is relatively larger, and thus BC radiative forcing does not respond linearly to emissions. The forcing efficiency of BC is generally higher over regions of southern and eastern Asia (increasing emissions) than over Europe and the USA (decreasing emissions); see Haywood and Ramaswamy (1998).

Figure 5a and b show the geographical distribution of the multi-model mean 1990–2015 radiative forcing of the direct
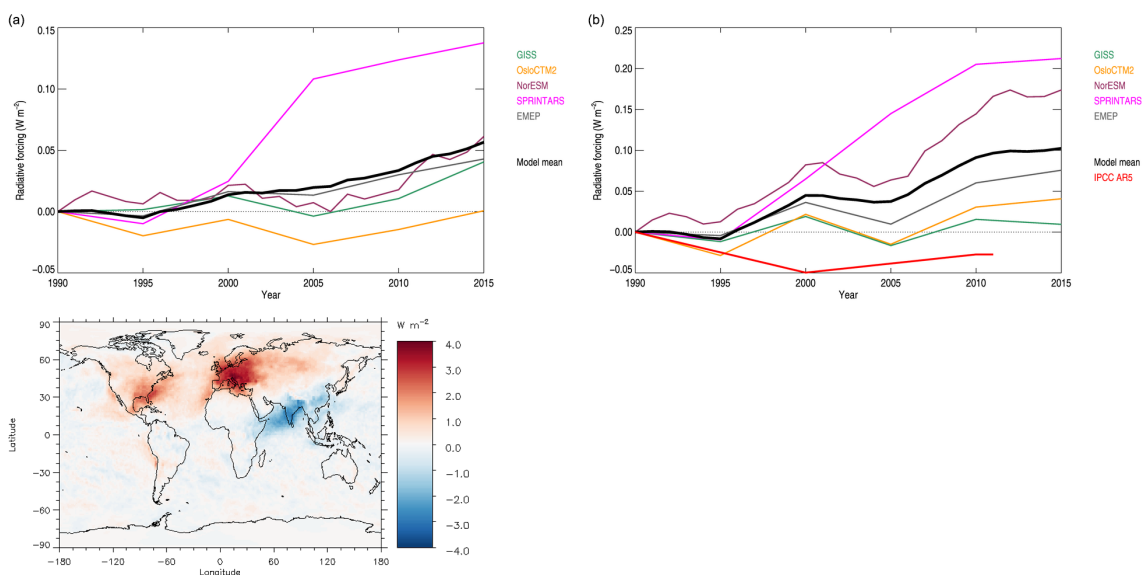
Figure 6. Radiative forcing ($W\,m^{-2}$) over the period 1990–2015 of the aerosol–cloud interaction for a subset of the models **(a)** and total aerosol effect **(b)**. The lower panel shows the geographical distribution of radiative forcing ($W\,m^{-2}$) of the multi-model mean total aerosol effect.

aerosol effect for sulfate and BC, respectively. Sulfate forcing changes by $+1$ to $+2\,W\,m^{-2}$ over the south-eastern USA and central Europe due to reduced abundances; it changes by -0.5 to $-1.5\,W\,m^{-2}$ over most of southern and eastern Asia. In other regions, the changes are minimal. The changes in the direct aerosol effect of BC are smaller in magnitude and opposite in sign: as much as $-0.3\,W\,m^{-2}$ over the USA and Europe and as much as $+0.3$ to $+1.0\,W\,m^{-2}$ over a broad region of the northern tropics and subtropics from Africa to eastern Asia. The multi-model direct aerosol effect forcing of POA is very similar to IPCC AR5 over the 1990–2010 period and is generally small in magnitude (Fig. 4c). To a small degree, the POA forcing acts to offset the positive forcing from BC and sulfate over the period 1990–2015. SOA are included in a few models, with forcing values over the 1990–2015 period generally of smaller magnitudes than POA. Three of the models have nitrate aerosols included, with a large range in the forcing over the period (Fig. 4d). The model range in nitrate forcing is presently larger than for other aerosol compounds (Myhre et al., 2013a; Shindell et al., 2013a). The strong nitrate forcing in the GISS model, which is likely too strong (Shindell et al., 2013a), explains the weak and negative total direct aerosol effect found here. Conversely, NorESM, showing the highest total direct aerosol forcing, is without nitrate aerosols. This model also shows the strongest BC forcing among the models in this study.

3.3 Aerosol–cloud interaction and total aerosol effect

A subset of five models were able to diagnose the forcing from aerosol–cloud interaction, with four models having a weak or slightly positive forcing and one model having

a large positive forcing; see Fig. 6a. In three of the models, rapid adjustments associated with aerosol–cloud interactions are simulated (i.e. in IPCC AR5 terms, they simulate an effective radiative forcing, or ERF), whereas in the two models OsloCTM2 and EMEP, the RF (changes only to the cloud albedo) was simulated. The differences in direct aerosol effect found here can largely be explained by differences in the individual aerosol components, but a disentangling of aerosol–cloud interaction is more complex and average differences across the models are not readily attributed (Boucher et al., 2013).

The forcing of the total aerosol effect (the combined aerosol–radiation and aerosol–cloud interaction) based on five models, excluding CESM-CAM5 and ECHAM, are shown in Fig. 6b. CESM-CAM5 and ECHAM both have direct aerosol effect very close to the model mean. All five models have a positive total aerosol effect at the end of the 1990–2015 time period, but the magnitudes vary substantially from near zero to $+0.2\,W\,m^{-2}$. The direct aerosol effect causes part of this spread, but the aerosol–cloud interaction is the major cause. Using the ECLIPSE emission data, we find a range similar to earlier studies, from weak to strongly positive total aerosol forcing (Kuhn et al., 2014), but that differs from the assessment of IPCC AR5, which had a negative total aerosol effect. Here, all models show a positive total aerosol forcing with a model mean of around $+0.1\,W\,m^{-2}$ ($0.10 \pm 0.08\,W\,m^{-2}$ with the uncertainty given as 1 standard deviation) for the 1990–2015 period. The semi-direct effect of BC and absorbing organic aerosol (OA) is included in the total aerosol effect for all the models, except NorESM. For two of the models (EMEP and OsloCTM2)

the semi-direct effect of BC is quantified to be -0.01 and $-0.03\,\mathrm{W\,m^{-2}}$ in 2015 and slightly stronger in 2010. These estimates were derived by the same method as in Hodne-brog et al. (2014) and Samset and Myhre (2015). The spatial distribution of the mean multi-model total aerosol forcing from aerosol changes over the 1990–2015 period is shown in Fig. 6c. The positive forcing dominates over most regions from a general reduction in the aerosol abundance, reaching a maximum of $4.0\,\mathrm{W\,m^{-2}}$ over Europe. Over southern and eastern Asia aerosol increases over the 1990–2015 period led to a negative forcing of $-3.0\,\mathrm{W\,m^{-2}}$.

3.4 Ozone forcing

The subset of five models that simulated ozone changes and their resulting radiative forcing all show positive RF over the entire time period. The multi-model mean forcing is twice the IPCC AR5 estimate; see Fig. 7. Three models that used fixed meteorology simulate a relatively stable ozone forcing increase, while the other two models show that interannual variability contributed noise to the calculation of this forcing. For the period from 1990 to 2015, the model mean forcing is $+0.06\,\mathrm{W\,m^{-2}}$, with a model range of the order of 50 around this value.

In addition to the shorter-lived ozone precursors of NO_x, CO and volatile organic compounds (VOCs) changes in the observed concentration of CH_4 are taken into account, except for the EMEP model. The ozone forcing estimate in IPCC AR5 was based on simulations in Stevenson et al. (2013) and for the period after 2005 on the Representative Concentration Pathways 4.5 (RCP4.5) scenario, which has a weaker increase in the forcing than the RCP8.5 scenario. The stronger ozone forcing in this work compared to IPCC AR5 is likely to be mainly caused by an increase in NO_x over the 1990–2010 period that is more than twice that in the emission data used in IPCC AR5; see Fig. 1. Changes in CO and VOCs are relatively small in the ECLIPSE data and those used for IPCC AR5. The smaller ozone trend from the EMEP model is partly due to their use of a constant CH_4 value in the trend calculations. Quantifying the contribution from the various individual ozone precursors is complicated due to nonlinearity (Stevenson et al., 2013).

4 Summary and conclusions

A suite of models simulated ozone and aerosol forcing over the 1990–2015 period, using new emission data from the European Union project ECLIPSE (Stohl et al., 2015). In areas where there are good and harmonised measurement networks (USA and Europe), the models generally reproduce observed large-scale surface trends in both compounds. Our key finding based on the updated model simulations is that there is stronger positive radiative forcing of aerosols and ozone over the past 25 years than reported in IPCC AR5. The global
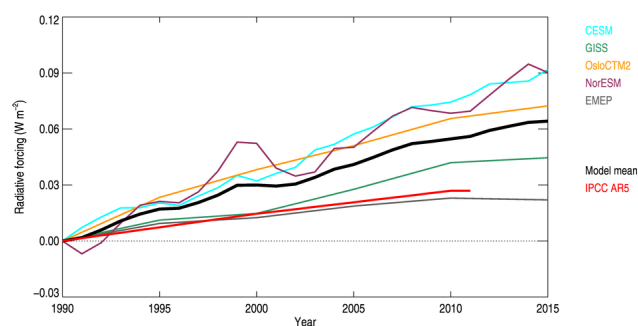

Figure 7. Radiative forcing ($\mathrm{W\,m^{-2}}$) due to the change in ozone over the period 1990–2015.

average total, multi-model ozone and aerosol forcing over the period 1990 to 2015 is almost $+0.2\,\mathrm{W\,m^{-2}}$. However, uncertainties are large, and the model diversity of aerosol–cloud interaction is especially pronounced. The model range in the direct aerosol effect can be explained by the individual aerosol components and the diversity in modelling these processes. The model range in the forcing of the direct aerosol effect of nitrate aerosols is large and needs further investigation. The model range in the direct aerosol effect of BC is also large, but recent progress on BC lifetime (Samset et al., 2014) and improved understanding of the importance of high-resolution modelling for reproducing surface BC measurements (Wang et al., 2014a) are likely to provide more constrained BC forcing estimates in the future. In a similar way, the aerosol–cloud interaction needs observational constraints for reduced model spread. The regional forcing of aerosol changes over the 1990–2015 period is large, with maximum values over Europe ($+4.0\,\mathrm{W\,m^{-2}}$) and south-eastern Asia ($-3.0\,\mathrm{W\,m^{-2}}$).

The dominant forcing mechanism over the 1990–2015 period is changes in the well-mixed greenhouse gases (WMGHGs). The global mean forcing due to CO_2 increased over this period by $0.66\,\mathrm{W\,m^{-2}}$ and forcing due to other WMGHGs rose by $0.16\,\mathrm{W\,m^{-2}}$ (see Supplement for further information of the calculations). Other anthropogenic forcing mechanisms had negligible overall changes between 1990 and 2015, though natural forcing of volcanic eruptions and solar irradiance changes had large changes during the period; see Prather et al. (2013) and particularly their Table AII.1.2. In particular, volcanic eruptions cause strong negative forcing on a timescale of a few years. The natural forcing due to volcanic and solar irradiance changes was found to be -0.16 (-0.27 to -0.06) $\mathrm{W\,m^{-2}}$ over the period 1998–2011 (Myhre et al., 2013b). Whereas previous studies indicated almost zero change in forcing of aerosol and ozone change, this study shows by using an updated emission inventory and multi-model simulations a forcing equal to 20 % of the WMGHG forcing.

5 Data availability

The data used are collected as part of national contributions to the EMEP programme (http://www.emep.int/) and through the IMPROVE programme. The EMEP data, covering Europe, are archived and available from the EMEP database EBAS (http://ebas.nilu.no/) located at NILU – Norwegian Institute for Air Research. EBAS is an infrastructure shared with other frameworks targeting atmospheric aerosol properties, such as the European Aerosols, Clouds, and Trace gases Research InfraStructure (ACTRIS), GAW-World Data Centre for Aerosols (GAW-WDCA) and GAW-World data centre for Reactive gases (GAW-WDCA). The data are public, traceable and well documented, with comprehensive metadata and version control.

IMPROVE is a collaborative association of state, tribal, and federal agencies and international partners. The IMPROVE data are public and available from the IMPROVE website (http://views.cira.colostate.edu/fed/DataWizard/Default.aspx).

Model data are available from Gunnar Myhre (gunnar.myhre@cicero.oslo.no).

The Supplement related to this article is available online at doi:10.5194/acp-17-2709-2017-supplement.

References

Amann, M., Klimont, Z., and Wagner, F.: Regional and Global Emissions of Air Pollutants: Recent Trends and Future Scenarios, Annu. Rev. Environ. Resour., 38, 31–55, 2013.

Barnes, E. A., Fiore, A. M., and Horowitz, L. W.: Detection of trends in surface ozone in the presence of climate variability, J. Geophys. Res.-Atmos., 121, 6112–6129, 2016.

Bentsen, M., Bethke, I., Debernard, J. B., Iversen, T., Kirkevåg, A., Seland, Ø., Drange, H., Roelandt, C., Seierstad, I. A., Hoose, C., and Kristjánsson, J. E.: The Norwegian Earth System Model, NorESM1-M – Part 1: Description and basic evaluation of the physical climate, Geosci. Model Dev., 6, 687–720, doi:10.5194/gmd-6-687-2013, 2013.

Boucher, O., Randall, D., Artaxo, P., Bretherton, C., Feingold, G., Forster, P., Kerminen, V.-M., Kondo, Y., Liao, H., Lohmann, U., Rasch, P., Satheesh, S. K., Sherwood, S., Stevens, B., and Zhang, X.-Y., Clouds and Aerosols, in: Climate Change 2013: The Physical Science Basis, Contribution of Working Group I to the Fifth Assessment Report of the Intergovernmental Panel on Climate Change, edited by: Stocker, T. F., Qin, D., Plattner, G.-K., Tignor, M., Allen, S. K., Boschung, J., Nauels, A., Xia, Y., Bex, V., and Midgley, P. M., Cambridge University Press, Cambridge, UK and New York, NY, USA, 571–657, 2013.

Crippa, M., Janssens-Maenhout, G., Dentener, F., Guizzardi, D., Sindelarova, K., Muntean, M., Van Dingenen, R., and Granier, C.: Forty years of improvements in European air quality: regional policy-industry interactions with global impacts, Atmos. Chem. Phys., 16, 3825–3841, doi:10.5194/acp-16-3825-2016, 2016.

Eyring, V., Bony, S., Meehl, G. A., Senior, C. A., Stevens, B., Stouffer, R. J., and Taylor, K. E.: Overview of the Coupled Model Intercomparison Project Phase 6 (CMIP6) experimental design and organization, Geosci. Model Dev., 9, 1937–1958, doi:10.5194/gmd-9-1937-2016, 2016.

Flato, G., Marotzke, J., Abiodun, B., Braconnot, P., Chou, S. C., Collins, W., Cox, P., Driouech, F., Emori, S., Eyring, V., Forest, C., Gleckler, P., Guilyardi, E., Jakob, C., Kattsov, V., Reason, C., and Rummukainen, M.: Evaluation of Climate Models, in: Climate Change 2013: The Physical Science Basis, Contribution of Working Group I to the Fifth Assessment Report of the Intergovernmental Panel on Climate Change, edited by: Stocker, T. F., Qin, D., Plattner, G.-K., Tignor, M., Allen, S. K., Boschung, J., Nauels, A., Xia, Y., Bex, V., and Midgley, P. M., Cambridge University Press, Cambridge, UK and New York, NY, USA, 741–866, 2013.

Forster, P. M. D. and Shine, K. P.: Radiative forcing and temperature trends from stratospheric ozone changes, J. Geophys. Res.-Atmos., 102, 10841–10855, 1997.

Fyfe, J. C., Meehl, G. A., England, M. H., Mann, M. E., Santer, B. D., Flato, G. M., Hawkins, E., Gillett, N. P., Xie, S.-P., Kosaka, Y., and Swart, N. C.: Making sense of the early-2000s warming slowdown, Nat. Clim. Change, 6, 224–228, 2016.

Granier, C., Bessagnet, B., Bond, T., D'Angiola, A., van der Gon, H. D., Frost, G. J., Heil, A., Kaiser, J. W., Kinne, S., Klimont, Z., Kloster, S., Lamarque, J. F., Liousse, C., Masui, T., Meleux, F., Mieville, A., Ohara, T., Raut, J. C., Riahi, K., Schultz, M. G., Smith, S. J., Thompson, A., van Aardenne, J., van der Werf, G. R., and van Vuuren, D. P.: Evolution of anthropogenic and biomass burning emissions of air pollutants at global and re-

gional scales during the 1980–2010 period, Climatic Change, 109, 163–190, 2011.

Hand, J. L., Copeland, S. A., Day, D. E., Dillner, A. M., Indresand, H., Malm, W. C., McDade, C. E., Moore, C. T., Pitchford, M. L., Schichtel, B. A., and Watson, J. G.: IMPROVE – Interagency Monitoring of Protected Visual Environments: Spatial and seasonal patterns and temporal variability of haze and its constituents in the United States, Report V, CIRA, Report ISSN: 0737-5352-87, http://vista.cira.colostate.edu/Improve/ (last access: February 2017), 2011.

Hand, J. L., Schichtel, B. A., Malm, W. C., Copeland, S., Molenar, J. V., Frank, N., and Pitchford, M.: Widespread reductions in haze across the United States from the early 1990s through 2011, Atmos. Environ., 94, 671–679, 2014.

Haywood, J. M. and Ramaswamy, V.: Global sensitivity studies of the direct radiative forcing due to anthropogenic sulfate and black carbon aerosols, J. Geophys. Res.-Atmos., 103, 6043–6058, 1998.

Haywood, J. M. and Shine, K. P.: Multi-spectral calculations of the direct radiative forcing of tropospheric sulphate and soot aerosols using a column model, Q. J. Roy. Meteorol. Soc., 123, 1907–1930, 1997.

Hodnebrog, Ø., Myhre, G., and Samset, B. H.: How shorter black carbon lifetime alters its climate effect, Nat. Commun., 5, 5065, doi:10.1038/ncomms6065, 2014.

Hoesly, R. M., Smith, S., Feng, L., Klimont, Z., Janssens-Maenhout, G., Pitkanen, T., Seibert, J. J., Vu, L., Andres, R. J., Bolt, R. M., Bond, T. C., Dawidowski, L., Kholod, N., Kurokawa, J., Li, M., Liu, L., Lu, Z., Moura, M. C. P., O'Rourke, R. R., and Zhang Q.: Historical (1750–2014) anthropogenic emissions of reactive gases and aerosols from the Community Emission Data System (CEDS), in preparation, 2017.

Iversen, T., Bentsen, M., Bethke, I., Debernard, J. B., Kirkevåg, A., Seland, Ø., Drange, H., Kristjansson, J. E., Medhaug, I., Sand, M., and Seierstad, I. A.: The Norwegian Earth System Model, NorESM1-M – Part 2: Climate response and scenario projections, Geosci. Model Dev., 6, 389–415, doi:10.5194/gmd-6-389-2013, 2013.

Karl, T. R., Arguez, A., Huang, B., Lawrimore, J. H., McMahon, J. R., Menne, M. J., Peterson, T. C., Vose, R. S., and Zhang, H.-M.: Possible artifacts of data biases in the recent global surface warming hiatus, Science, 348, 1469–1472, 2015.

Kaufman, Y. J., Tanre, D., and Boucher, O.: A satellite view of aerosols in the climate system, Nature, 419, 215–223, 2002.

Kirkevåg, A., Iversen, T., Seland, Ø., Hoose, C., Kristjánsson, J. E., Struthers, H., Ekman, A. M. L., Ghan, S., Griesfeller, J., Nilsson, E. D., and Schulz, M.: Aerosol–climate interactions in the Norwegian Earth System Model – NorESM1-M, Geosci. Model Dev., 6, 207–244, doi:10.5194/gmd-6-207-2013, 2013.

Klimont, Z., Smith, S. J., and Cofala, J.: The last decade of global anthropogenic sulfur dioxide: 2000–2011 emissions, Environ. Res. Lett., 8, 014003, doi:10.1088/1748-9326/8/1/014003, 2013.

Klimont, Z., Kupiainen, K., Heyes, C., Purohit, P., Cofala, J., Rafaj, P., Borken-Kleefeld, J., and Schöpp, W.: Global anthropogenic emissions of particulate matter including black carbon, Atmos. Chem. Phys. Discuss., doi:10.5194/acp-2016-880, in review, 2016.

Kuhn, T., Partanen, A. I., Laakso, A., Lu, Z., Bergman, T., Mikkonen, S., Kokkola, H., Korhonen, H., Raisanen, P., Streets, D. G., Romakkaniemi, S., and Laaksonen, A.: Climate impacts of changing aerosol emissions since 1996, Geophys. Res. Lett., 41, 4711–4718, 2014.

Lacis, A. A., Wuebbles, D. J., and Logan, J. A.: Radiative forcing of climate by changes in the vertical distribution of ozone, J. Geophys. Res.-Atmos., 95, 9971–9981, 1990.

Lamarque, J.-F., Bond, T. C., Eyring, V., Granier, C., Heil, A., Klimont, Z., Lee, D., Liousse, C., Mieville, A., Owen, B., Schultz, M. G., Shindell, D., Smith, S. J., Stehfest, E., Van Aardenne, J., Cooper, O. R., Kainuma, M., Mahowald, N., McConnell, J. R., Naik, V., Riahi, K., and van Vuuren, D. P.: Historical (1850–2000) gridded anthropogenic and biomass burning emissions of reactive gases and aerosols: methodology and application, Atmos. Chem. Phys., 10, 7017–7039, doi:10.5194/acp-10-7017-2010, 2010.

Liu, X., Easter, R. C., Ghan, S. J., Zaveri, R., Rasch, P., Shi, X., Lamarque, J.-F., Gettelman, A., Morrison, H., Vitt, F., Conley, A., Park, S., Neale, R., Hannay, C., Ekman, A. M. L., Hess, P., Mahowald, N., Collins, W., Iacono, M. J., Bretherton, C. S., Flanner, M. G., and Mitchell, D.: Toward a minimal representation of aerosols in climate models: description and evaluation in the Community Atmosphere Model CAM5, Geosci. Model Dev., 5, 709–739, doi:10.5194/gmd-5-709-2012, 2012.

Liu, X. H., Penner, J. E., Das, B. Y., Bergmann, D., Rodriguez, J. M., Strahan, S., Wang, M. H., and Feng, Y.: Uncertainties in global aerosol simulations: Assessment using three meteorological data sets, J. Geophys. Res.-Atmos., 112, D11212, doi:10.1029/2006JD008216, 2007.

MacIntosh, C. R., Allan, R. P., Baker, L. H., Bellouin, N., Collins, W., Mousavi, Z., and Shine, K. P.: Contrasting fast precipitation responses to tropospheric and stratospheric ozone forcing, Geophys. Res. Lett., 43, 1263–1271, 2016.

Marotzke, J. and Forster, P. M.: Forcing, feedback and internal variability in global temperature trends, Nature, 517, 565–570, 2015.

Murphy, D. M.: Little net clear-sky radiative forcing from recent regional redistribution of aerosols, Nat. Geosci., 6, 258–262, 2013.

Myhre, G., Berglen, T. F., Johnsrud, M., Hoyle, C. R., Berntsen, T. K., Christopher, S. A., Fahey, D. W., Isaksen, I. S. A., Jones, T. A., Kahn, R. A., Loeb, N., Quinn, P., Remer, L., Schwarz, J. P., and Yttri, K. E.: Modelled radiative forcing of the direct aerosol effect with multi-observation evaluation, Atmos. Chem. Phys., 9, 1365–1392, doi:10.5194/acp-9-1365-2009, 2009.

Myhre, G., Samset, B. H., Schulz, M., Balkanski, Y., Bauer, S., Berntsen, T. K., Bian, H., Bellouin, N., Chin, M., Diehl, T., Easter, R. C., Feichter, J., Ghan, S. J., Hauglustaine, D., Iversen, T., Kinne, S., Kirkevåg, A., Lamarque, J.-F., Lin, G., Liu, X., Lund, M. T., Luo, G., Ma, X., van Noije, T., Penner, J. E., Rasch, P. J., Ruiz, A., Seland, Ø., Skeie, R. B., Stier, P., Takemura, T., Tsigaridis, K., Wang, P., Wang, Z., Xu, L., Yu, H., Yu, F., Yoon, J.-H., Zhang, K., Zhang, H., and Zhou, C.: Radiative forcing of the direct aerosol effect from AeroCom Phase II simulations, Atmos. Chem. Phys., 13, 1853–1877, doi:10.5194/acp-13-1853-2013, 2013a.

Myhre, G., Shindell, D., Bréon, F.-M., Collins, W., Fuglestvedt, J., Huang, J., Koch, D., Lamarque, J.-F., Lee, D., Mendoza, B., Nakajima, T., Robock, A., Stephens, G., Takemura, T., and Zhang, H., Anthropogenic and Natural Radiative Forcing, in: Cli-

mate Change 2013: The Physical Science Basis, Contribution of Working Group I to the Fifth Assessment Report of the Intergovernmental Panel on Climate Change, edited by: Stocker, T. F., Qin, D., Plattner, G.-K., Tignor, M., Allen, S. K., Boschung, J., Nauels, A., Xia, Y., Bex, V., and Midgley, P. M., Cambridge University Press, Cambridge, UK and New York, NY, USA, 659–740, 2013b.

Neale, R. B., Gettelman, A., Park, S., Chen, C., Lauritzen, P. H., Williamson, D. L., Conley, A. J., Kinnison, D., Marsh, D., Smith, A. K., Vitt, F., Garcia, R., Lamarque, J. F., Mills, M., Tilmes, S., Morrison, H., Cameron-Smith, P., Collins, W. D., Iacono, M., Easter, R. C., Liu, X., Ghan, S., Rasch, P., and Taylor, M. A.: Description of the NCAR Community Atmosphere Model (CAM 5.0), NCAR Technical Report, NCAR/TN-486+STR, National Center for Atmospheric Research – NCAR, Boulder, Colorado, 2010.

Nieves, V., Willis, J. K., and Patzert, W. C.: Recent hiatus caused by decadal shift in Indo-Pacific heating, Science, 349, 532–535, 2015.

Prather, M., Flato, G., Friedlingstein, P., Jones, C., Lamarque, J.-F., Liao, H., and Rasch, P.: IPCC 2013: Annex II: Climate System Scenario Tables, in: Climate Change 2013: The Physical Science Basis, Contribution of Working Group I to the Fifth Assessment Report of the Intergovernmental Panel on Climate Change, edited by: Stocker, T. F., Qin, D., Plattner, G.-K., Tignor, M., Allen, S. K., Boschung, J., Nauels, A., Xia, Y., Bex, V., and Midgley, P. M., Cambridge University Press, Cambridge, UK and New York, NY, USA, 1395–1445, 2013.

Samset, B. H. and Myhre, G.: Climate response to externally mixed black carbon as a function of altitude, J. Geophys. Res.- Atmos., 120, 2913–2927, 2015.

Samset, B. H., Myhre, G., Schulz, M., Balkanski, Y., Bauer, S., Berntsen, T. K., Bian, H., Bellouin, N., Diehl, T., Easter, R. C., Ghan, S. J., Iversen, T., Kinne, S., Kirkevåg, A., Lamarque, J.-F., Lin, G., Liu, X., Penner, J. E., Seland, Ø., Skeie, R. B., Stier, P., Takemura, T., Tsigaridis, K., and Zhang, K.: Black carbon vertical profiles strongly affect its radiative forcing uncertainty, Atmos. Chem. Phys., 13, 2423–2434, doi:10.5194/acp-13-2423-2013, 2013.

Samset, B. H., Myhre, G., Herber, A., Kondo, Y., Li, S.-M., Moteki, N., Koike, M., Oshima, N., Schwarz, J. P., Balkanski, Y., Bauer, S. E., Bellouin, N., Berntsen, T. K., Bian, H., Chin, M., Diehl, T., Easter, R. C., Ghan, S. J., Iversen, T., Kirkevåg, A., Lamarque, J.-F., Lin, G., Liu, X., Penner, J. E., Schulz, M., Seland, Ø., Skeie, R. B., Stier, P., Takemura, T., Tsigaridis, K., and Zhang, K.: Modelled black carbon radiative forcing and atmospheric lifetime in AeroCom Phase II constrained by aircraft observations, Atmos. Chem. Phys., 14, 12465–12477, doi:10.5194/acp-14-12465-2014, 2014.

Sand, M., Samset, B. H., Balkanski, Y., Bauer, S., Bellouin, N., Berntsen, T. K., Bian, H., Chin, M., Diehl, T., Easter, R., Ghan, S. J., Iversen, T., Kirkevåg, A., Lamarque, J.-F., Lin, G., Liu, X., Luo, G., Myhre, G., van Noije, T., Penner, J. E., Schulz, M., Seland, Ø., Skeie, R. B., Stier, P., Takemura, T., Tsigaridis, K., Yu, F., Zhang, K., and Zhang, H.: Aerosols at the Poles: An AeroCom Phase II multi-model evaluation, Atmos. Chem. Phys. Discuss., doi:10.5194/acp-2016-1120, in review, 2017.

Schmidt, G. A., Kelley, M., Nazarenko, L., Ruedy, R., Russell, G. L., Aleinov, I., Bauer, M., Bauer, S. E., Bhat, M. K., Bleck, R.,

Canuto, V., Chen, Y.-H., Cheng, Y., Clune, T. L., Del Genio, A., de Fainchtein, R., Faluvegi, G., Hansen, J. E., Healy, R. J., Kiang, N. Y., Koch, D., Lacis, A. A., LeGrande, A. N., Lerner, J., Lo, K. K., Matthews, E. E., Menon, S., Miller, R. L., Oinas, V., Oloso, A. O., Perlwitz, J. P., Puma, M. J., Putman, W. M., Rind, D., Romanou, A., Sato, M., Shindell, D. T., Sun, S., Syed, R. A., Tausnev, N., Tsigaridis, K., Unger, N., Voulgarakis, A., Yao, M.-S. and Zhang, J.: Configuration and assessment of the GISS ModelE2 contributions to the CMIP5 archive, J. Adv. Model. Earth Syst., 6, 141–184, 2014a.

Schmidt, G. A., Shindell, D. T., and Tsigaridis, K.: Reconciling warming trends, Nat. Geosci., 7, 158–160, 2014b.

Schnell, J. L., Holmes, C. D., Jangam, A., and Prather, M. J.: Skill in forecasting extreme ozone pollution episodes with a global atmospheric chemistry model, Atmos. Chem. Phys., 14, 7721–7739, doi:10.5194/acp-14-7721-2014, 2014.

Schnell, J. L., Prather, M. J., Josse, B., Naik, V., Horowitz, L. W., Cameron-Smith, P., Bergmann, D., Zeng, G., Plummer, D. A., Sudo, K., Nagashima, T., Shindell, D. T., Faluvegi, G., and Strode, S. A.: Use of North American and European air quality networks to evaluate global chemistry–climate modeling of surface ozone, Atmos. Chem. Phys., 15, 10581–10596, doi:10.5194/acp-15-10581-2015, 2015.

Schutgens, N. A. J., Gryspeerdt, E., Weigum, N., Tsyro, S., Goto, D., Schulz, M., and Stier, P.: Will a perfect model agree with perfect observations? The impact of spatial sampling, Atmos. Chem. Phys., 16, 6335–6353, doi:10.5194/acp-16-6335-2016, 2016.

Shindell, D. T., Lamarque, J.-F., Schulz, M., Flanner, M., Jiao, C., Chin, M., Young, P. J., Lee, Y. H., Rotstayn, L., Mahowald, N., Milly, G., Faluvegi, G., Balkanski, Y., Collins, W. J., Conley, A. J., Dalsoren, S., Easter, R., Ghan, S., Horowitz, L., Liu, X., Myhre, G., Nagashima, T., Naik, V., Rumbold, S. T., Skeie, R., Sudo, K., Szopa, S., Takemura, T., Voulgarakis, A., Yoon, J.-H., and Lo, F.: Radiative forcing in the ACCMIP historical and future climate simulations, Atmos. Chem. Phys., 13, 2939–2974, doi:10.5194/acp-13-2939-2013, 2013a.

Shindell, D. T., Pechony, O., Voulgarakis, A., Faluvegi, G., Nazarenko, L., Lamarque, J.-F., Bowman, K., Milly, G., Kovari, B., Ruedy, R., and Schmidt, G. A.: Interactive ozone and methane chemistry in GISS-E2 historical and future climate simulations, Atmos. Chem. Phys., 13, 2653–2689, doi:10.5194/acp-13-2653-2013, 2013b.

Simpson, D., Benedictow, A., Berge, H., Bergström, R., Emberson, L. D., Fagerli, H., Flechard, C. R., Hayman, G. D., Gauss, M., Jonson, J. E., Jenkin, M. E., Nyíri, A., Richter, C., Semeena, V. S., Tsyro, S., Tuovinen, J.-P., Valdebenito, Á., and Wind, P.: The EMEP MSC-W chemical transport model – technical description, Atmos. Chem. Phys., 12, 7825–7865, doi:10.5194/acp-12-7825-2012, 2012.

Skeie, R. B., Berntsen, T. K., Myhre, G., Tanaka, K., Kvalevåg, M. M., and Hoyle, C. R.: Anthropogenic radiative forcing time series from pre-industrial times until 2010, Atmos. Chem. Phys., 11, 11827–11857, doi:10.5194/acp-11-11827-2011, 2011.

Solomon, S., Daniel, J. S., Neely, R. R., III, Vernier, J. P., Dutton, E. G., and Thomason, L. W.: The Persistently Variable "Background" Stratospheric Aerosol Layer and Global Climate Change, Science, 333, 866–870, 2011.

Stevens, B., Giorgetta, M., Esch, M., Mauritsen, T., Crueger, T., Rast, S., Salzmann, M., Schmidt, H., Bader, J., Block, K.,

Brokopf, R., Fast, I., Kinne, S., Kornblueh, L., Lohmann, U., Pincus, R., Reichler, T., and Roeckner, E.: Atmospheric component of the MPI-M Earth System Model: ECHAM6, J. Adv. Model. Earth Syst., 5, 146–172, 2013.

Stevenson, D. S., Young, P. J., Naik, V., Lamarque, J.-F., Shindell, D. T., Voulgarakis, A., Skeie, R. B., Dalsoren, S. B., Myhre, G., Berntsen, T. K., Folberth, G. A., Rumbold, S. T., Collins, W. J., MacKenzie, I. A., Doherty, R. M., Zeng, G., van Noije, T. P. C., Strunk, A., Bergmann, D., Cameron-Smith, P., Plummer, D. A., Strode, S. A., Horowitz, L., Lee, Y. H., Szopa, S., Sudo, K., Nagashima, T., Josse, B., Cionni, I., Righi, M., Eyring, V., Conley, A., Bowman, K. W., Wild, O., and Archibald, A.: Tropospheric ozone changes, radiative forcing and attribution to emissions in the Atmospheric Chemistry and Climate Model Intercomparison Project (ACCMIP), Atmos. Chem. Phys., 13, 3063–3085, doi:10.5194/acp-13-3063-2013, 2013.

Stier, P., Schutgens, N. A. J., Bellouin, N., Bian, H., Boucher, O., Chin, M., Ghan, S., Huneeus, N., Kinne, S., Lin, G., Ma, X., Myhre, G., Penner, J. E., Randles, C. A., Samset, B., Schulz, M., Takemura, T., Yu, F., Yu, H., and Zhou, C.: Host model uncertainties in aerosol radiative forcing estimates: results from the AeroCom Prescribed intercomparison study, Atmos. Chem. Phys., 13, 3245–3270, doi:10.5194/acp-13-3245-2013, 2013.

Stohl, A., Aamaas, B., Amann, M., Baker, L. H., Bellouin, N., Berntsen, T. K., Boucher, O., Cherian, R., Collins, W., Daskalakis, N., Dusinska, M., Eckhardt, S., Fuglestvedt, J. S., Harju, M., Heyes, C., Hodnebrog, Ø., Hao, J., Im, U., Kanakidou, M., Klimont, Z., Kupiainen, K., Law, K. S., Lund, M. T., Maas, R., MacIntosh, C. R., Myhre, G., Myriokefalitakis, S., Olivié, D., Quaas, J., Quennehen, B., Raut, J.-C., Rumbold, S. T., Samset, B. H., Schulz, M., Seland, Ø., Shine, K. P., Skeie, R. B., Wang, S., Yttri, K. E., and Zhu, T.: Evaluating the climate and air quality impacts of short-lived pollutants, Atmos. Chem. Phys., 15, 10529–10566, doi:10.5194/acp-15-10529-2015, 2015.

Takemura, T., Nozawa, T., Emori, S., Nakajima, T. Y., and Nakajima, T.: Simulation of climate response to aerosol direct and indirect effects with aerosol transport-radiation model, J. Geophys. Res.-Atmos., 110, D02202, doi:10.1029/2004jd005029, 2005.

Takemura, T., Egashira, M., Matsuzawa, K., Ichijo, H., O'ishi, R., and Abe-Ouchi, A.: A simulation of the global distribution and radiative forcing of soil dust aerosols at the Last Glacial Maximum, Atmos. Chem. Phys., 9, 3061–3073, doi:10.5194/acp-9-3061-2009, 2009.

Tørseth, K., Aas, W., Breivik, K., Fjæraa, A. M., Fiebig, M., Hjellbrekke, A. G., Lund Myhre, C., Solberg, S., and Yttri, K. E.: Introduction to the European Monitoring and Evaluation Programme (EMEP) and observed atmospheric composition change during 972–2009, Atmos. Chem. Phys., 12, 5447–5481, doi:10.5194/acp-12-5447-2012, 2012.

Wang, H., Easter, R. C., Rasch, P. J., Wang, M., Liu, X., Ghan, S. J., Qian, Y., Yoon, J.-H., Ma, P.-L., and Vinoj, V.: Sensitivity of remote aerosol distributions to representation of cloud–aerosol interactions in a global climate model, Geosci. Model Dev., 6, 765–782, doi:10.5194/gmd-6-765-2013, 2013.

Wang, R., Tao, S., Balkanski, Y., Ciais, P., Boucher, O., Liu, J. F., Piao, S. L., Shen, H. Z., Vuolo, M. R., Valari, M., Chen, H., Chen, Y. C., Cozic, A., Huang, Y., Li, B. G., Li, W., Shen, G. F., Wang, B., and Zhang, Y. Y.: Exposure to ambient black carbon derived from a unique inventory and high-resolution model, P. Natl. Acad. Sci. USA, 111, 2459–2463, 2014a.

Wang, R., Tao, S., Shen, H. Z., Huang, Y., Chen, H., Balkanski, Y., Boucher, O., Ciais, P., Shen, G. F., Li, W., Zhang, Y. Y., Chen, Y. C., Lin, N., Su, S., Li, B. G., Liu, J. F., and Liu, W. X.: Trend in Global Black Carbon Emissions from 1960 to 2007, Environ. Sci. Technol., 48, 6780–6787, 2014b.

Zhang, K., O'Donnell, D., Kazil, J., Stier, P., Kinne, S., Lohmann, U., Ferrachat, S., Croft, B., Quaas, J., Wan, H., Rast, S., and Feichter, J.: The global aerosol-climate model ECHAM-HAM, version 2: sensitivity to improvements in process representations, Atmos. Chem. Phys., 12, 8911–8949, doi:10.5194/acp-12-8911-2012, 2012.